Available online at www.sciencedirect.com
SCIENCE DIRECT®
Journal of Power Sources 129 (2004) 14–19
JOURNAL OF POWER SOURCES
www.elsevier.com/locate/jpowsour

Improved lithium manganese oxide spinel/graphite Li-ion cells for high-power applications

K. Amine*, J. Liu, S. Kang, I. Belharouak, Y. Hyung, D. Vissers, G. Henriksen

Electrochemical Technology Program, Chemical Engineering Division, Argonne National Laboratory, Argonne, IL 60439, USA

Abstract

The degradation mechanism of lithium manganese oxide spinel/graphite Li-ion cells using $LiPF_6$-based electrolyte was investigated by a Mn-dissolution approach during high-temperature storage, and by ac impedance measurement using a reference electrode-equipped cell. Through these studies, we confirmed that Mn ions were dissolved from the spinel cathode in the electrolyte and were subsequently reduced on the lithiated graphite electrode surface, due to the chemical activity of the lithiated graphite, and caused a huge increase in the charge-transfer impedance at the graphite/electrolyte interface, which consequently deteriorated cell performance. To overcome the significant degradation of the spinel/graphite Li-ion cells, we investigated a new electrolyte system using lithium bisoxalatoborate (LiBoB, $LiB(C_2O_4)_2$) salt not having fluorine species in its chemical structure. Superior cycling performance at elevated temperature was observed with the spinel/graphite cells using LiBoB-based electrolyte, which is attributed to the inert chemical structure of LiBoB that does not generate HF. Mn-ion leaching experiments showed that almost no Mn ions were dissolved from the spinel powder after 55 °C storage for 4 weeks. Through optimization of organic solvents for the LiBoB salt, we developed an advanced Li-ion cell chemistry that used lithium manganese oxide spinel, 0.7 M LiBoB/EC:PC:DMC (1:1:3), and graphite as the cathode, electrolyte, and anode, respectively. This cell provides excellent power characteristics, good calendar life, and improved thermal safety for hybrid electric vehicle applications.

Keywords: High-power Li-ion cell; Lithium manganese oxide spinel; LiBoB; Mn dissolution; Capacity fading

1. Introduction

High-power lithium-ion batteries are promising alternatives to the nickel metal hydride batteries currently being used for energy storage in hybrid electric vehicles (HEVs). In the last few years, Argonne National Laboratory (ANL) has developed high-power Li-ion cell chemistries with lithium nickel cobalt oxide (with and without Al doping) and graphite as the cathode and anode, respectively. This work was carried out under the FreedomCAR Partnership. Although the cell chemistries with the lithium nickel cobalt oxide cathodes meet the power requirements for HEV applications [1], the Li-ion systems using $LiNi_{0.8}Co_{0.2}O_2$-based cathodes still have major concerns related to calendar life, safety, and cost. To address these concerns, ANL is investigating the possibility of replacing the lithium nickel oxide cathode system with lithium manganese oxide spinel.

Lithium manganese oxide spinel (LMOS) is very attractive for HEV batteries in many aspects, such as low cost, thermal safety due to the superior stability of Mn^{4+} at the fully charged state, and excellent rate capability due to its three-dimensional framework structure. In spite of these advantages, however, LMOS is not currently accepted by battery manufacturers due to its severe capacity fading during cycling at elevated temperatures (ETs), which is generally attributed to Mn dissolution from the spinel cathode induced by HF acid generated by fluorine from fluorinated anions (PF_6^-) and protons from water impurities [2–4]. As will be shown later, the capacity fading of LMOS at ET is strikingly larger in full Li-ion cells (versus graphite) than in half cells (versus Li metal). Therefore, improvement of the high-temperature cycling performance of LMOS/graphite cells, either by appropriate chemical doping of the LMOS or by developing alternative electrolyte systems that do not produce an acidic environment, is needed to ensure its use for commercial Li-ion batteries.

In this work, we investigated the capacity fading mechanism of LMOS/graphite Li-ion cells by high-temperature storage, galvanostatic cycling, and impedance measurement experiments. The degradation of the Li-ion cells was found to originate from Mn reduction at the surface of the graphite anode. In this article, we also report our research efforts to develop novel electrolyte systems that suppress Mn dissolution from the spinel electrode and significantly

* Corresponding author. Tel.: +1-301-394-0340; fax: +1-301-394-0273.
E-mail addresses: rjow@arl.army.mil, amine@cmt.anl.gov (K. Amine).

0378-7753/$ – see front matter © 2003 Published by Elsevier B.V.
doi:10.1016/j.jpowsour.2003.11.007

improve the high-temperature cycling performance. This paper describes the performance of the LMOS/graphite Li-ion cell system using a new lithium bisoxalatoborate (LiBoB, $LiB(C_2O_4)_2$)-based electrolyte.

2. Experimental

Stabilized lithium manganese oxide spinel, $Li_{1.06}Mn_{1.95}Al_{0.05}O_4$ (SLMOS), was used as the cathode material throughout this work. This material was prepared by mixing stoichiometric amount of MnO_2, Al_2O_3 and LiOH and heating the mix at 780 °C. After several recalcination processes, X-ray diffraction shows that the material has a pure spinel phase. The electrolytes used were either $LiPF_6$ or LiBoB dissolved in various organic solvents, such as ethylene carbonate (EC), diethyl carbonate (DEC), propylene carbonate (PC), and dimethyl carbonate (DMC).

For the Mn leaching experiments, we placed 0.5 g samples of spinel powder in 10 ml electrolyte solutions and then stored them at 55 °C for 4 weeks. The spinel powders after 4 weeks were then filtered from the electrolyte, and the manganese contents of the electrolytes were analyzed using an inductively coupled plasma (ICP) spectrometer.

To evaluate the electrochemical properties of the LMOS/graphite Li-ion cells, galvanostatic cycling, hybrid pulse-power characterization (HPPC) tests, and accelerated aging tests were carried out. The cathode paste was made of 80:10:10 spinel powder, carbon black, and polyvinylidene difluoride (PVDF), respectively, and was coated onto aluminum foil. The negative electrode was either metallic lithium or graphite coated on copper foil. The HPPC tests were carried out at room temperature using a test fixture with an electrode surface area of 15.5 cm^2 for both the positive and negative electrodes. The HPPC tests were performed in accordance with the FreedomCAR battery test manual [5]. This test is intended to determine dynamic power capability over the battery's useable charge and voltage range, using a test profile that incorporates both discharge and regen pulses. The primary objective of this test is to establish, as a function of the depth of discharge (DOD), (1) V_{min} cell discharge power capability at the end of an 18 s discharge current pulse and (2) the V_{max} cell regen power capability over the first 2 s of a trapezoidal regen current pulse. Secondary objectives are to derive from the voltage-response curves the fixed cell impedance and cell polarization impedance as a function of time with sufficient resolution to reliably establish cell voltage response time constants during discharge, rest, and regen operating regimes. The accelerated aging tests were conducted as follows: after the initial formation cycles, the cells were charged to 4 V and stored at 55 °C. Every couple of days, the cells were cooled down to room temperature, and the area-specific impedance (ASI) and capacity were measured. The ASI values were determined by $A\Delta V/I$, where A is the cross-sectional area of the cathode, ΔV the voltage variation during current interruption for 30 s at each SOC, and I the current applied during galvanostatic cycling. By repeating the above steps, the changes in cell impedance and capacity with aging time were monitored and recorded.

Cells with reference electrodes (RE) were used to investigate the major sources of impedance rise during the high-temperature cycling. The RE utilized a Li–Sn alloy on the tip of a 25 μm thick Cu wire. First, the tip of Cu wire was electroplated with 1 μm of tin (Sn) layer. The wire was then placed between two separator films which were sandwiched by the positive and the negative electrodes. The Li–Sn reference electrode was then formed by charging the tin layer at the tip of the wire with small amount of lithium from the positive electrode. Once the Li–Sn electrode reaches 0.6 V versus Li/Li^+, the charging is discontinued and the Li–Sn reference electrode is formed. The experimental details of RE cell construction are described elsewhere [6]. The RE cell was galvanostatically cycled at 55 °C; after 25 cycles, the impedances of the RE cell were measured between the cathode and the RE, the anode and the RE, and the cathode and the anode in the frequency range 10 mHz to 100 kHz.

Differential scanning calorimetry (DSC) experiments were conducted on the SLMOS cathode charged to 4.2 V (versus metallic Li). The data were acquired using a Perkin-Elmer Pyris 1 DSC at a scan rate of 10 °C/min over the temperature range of 50–350 °C. Details of the DSC experiments are described elsewhere [7].

3. Results and discussion

Fig. 1 shows the concentration of Mn ions after 4 weeks of storage of SLMOS powder in $LiPF_6$/EC:DEC (1:1) electrolyte at 55 °C. The Mn-ion concentration from stoichiometric LMOS ($LiMn_2O_4$) powder under the same experimental condition is also shown in Fig. 1 for comparison.

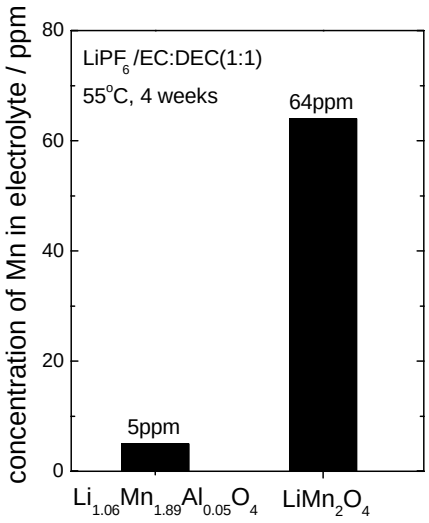

Fig. 1. Concentration of Mn dissolved from SLMOS and $LiMn_2O_4$ powders stored in $LiPF_6$/EC:DEC (1:1) electrolyte at 55 °C for 4 weeks.

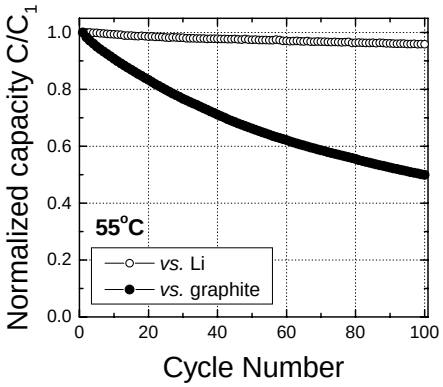

Fig. 2. Normalized discharge capacity characteristics vs. cycle number of SLMOS/Li (open circles) and SLMOS/graphite (closed circles) cells cycled at 55 °C. The electrolyte was 1 M $LiPF_6$/EC:DEC (1:1). C_1 denotes the first discharge capacity.

The dissolution of Mn ions from spinel into the electrolyte is generally attributed to the disproportionation reaction ($2Mn^{3+} \rightarrow Mn^{4+} + Mn^{2+}$) on the surface of the spinel electrode that is accelerated by the attack of acid such as HF in the $LiPF_6$-based electrolyte [8,9]. The Mn^{2+} ions are then readily dissolved into the organic liquid electrolyte. The superior stability of SLMOS powder against Mn dissolution is thought to originate from the increased average Mn valence (>+3.5) through Li- and Al-doping, thus suppressing or significantly reducing the disproportionation reaction.

The galvanostatic cycling results of SLMOS/Li and SLMOS/graphite cells cycled at 55 °C are shown in Fig. 2. The SLMOS/Li cell exhibited relatively good cycling performance (85% capacity retention after 100 cycles), as was expected from the Mn-dissolution experiment shown in Fig. 1. Surprisingly, however, the SLMOS still exhibited severe capacity fading (50% capacity retention after 100 cycles) in the full Li-ion cell despite the limited Mn dissolution (less than 5 ppm).

The results in Fig. 2 indicate that even small amounts of Mn present in the electrolyte could impact in a negative way the cycling performance of the LMOS/graphite Li-ion cells. To investigate the contribution of each electrode to cell degradation, we performed ac impedance measurements with the RE cell, the results of which are given in Fig. 3. The ac impedance was measured after one formation cycle at RT (Fig. 3(a)) and after 25 cycles at 55 °C (Fig. 3(b)). The open-circuit voltages at which the impedance was measured were 3.91 and 3.95 V, respectively. At the initial stage of cycling, the impedance of the negative electrode was much smaller than that of the positive electrode, as seen in Fig. 3(a), so that the latter mostly contributed to the overall impedance of the full cell (denoted as "Full" in Fig. 3). After 25 cycles at 55 °C, however, the impedance of the negative electrode significantly increased and overwhelmed the impedance of the positive electrode. The results in Fig. 3 suggest that the significant interfacial impedance increase of the graphite anode is the

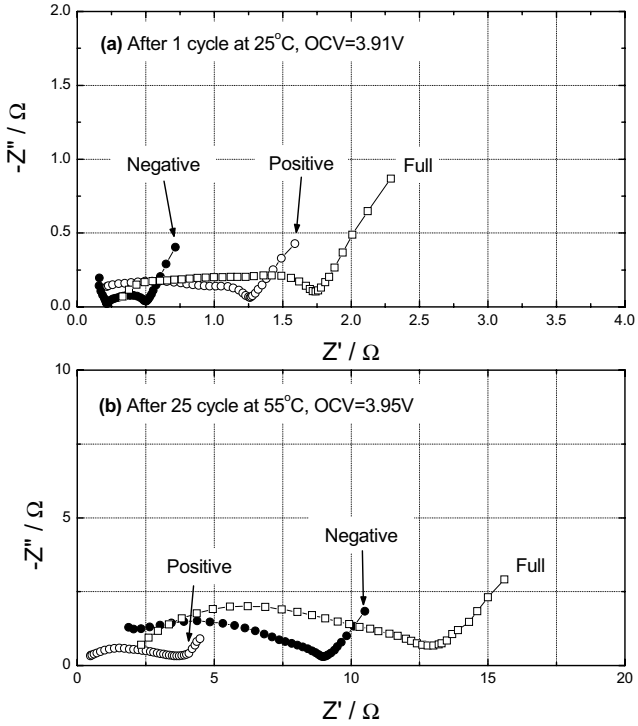

Fig. 3. Impedance of SLMOS/graphite cell with Li–Sn alloy reference electrode (RE): (a) after 1 cycle at 25 °C and at the OCV of 3.91 V; (b) after 25 cycles at 55 °C and at the OCV of 3.95 V. "Positive" and "Negative" denote impedances measured between the positive and negative electrodes and the RE, respectively. The full-cell impedance was measured between the positive and negative electrodes.

main source of the cell degradation. This result is quite opposite to the behavior of the $Li(Ni_{0.8}Co_{0.2})O_2$/graphite high-power cell [4]. The impedance of the graphite anode in the $Li(Ni_{0.8}Co_{0.2})O_2$/graphite cell showed a very limited increase after aging (at 70 °C for 2 weeks), whereas a huge impedance rise was observed in the $Li(Ni_{0.8}Co_{0.2})O_2$ cathode. We believe that the huge increase of negative electrode impedance in our case was caused by a surface reaction at the carbon electrode induced by the reduction of Mn ions (present in the electrolyte) at the carbon surface.

From the results in Figs. 1–3, it appears that the degradation of the LMOS/graphite cells occurs as follows: step I—disproportionation and dissolution of the Mn ions from the spinel powder into the electrolyte; step II—migration of the dissolved Mn ions to the graphite anode; step III—reduction of the Mn ions on the anode surface due to the chemical activity of the graphite; step IV—increase of charge-transfer impedance at the graphite/electrolyte interface. Consequently, the capacity fading problem of LMOS/graphite Li-ion cells cannot be avoided as long as Mn dissolution takes place, even though the dissolved amount is very small. It is well known that Mn dissolution from spinel powder is induced by HF acid generated by fluorine from fluorinated anions (PF_6^-) and protons from water impurities [2–4]. For successful commercialization of LMOS/graphite Li-ion cells, therefore, it is highly impor-

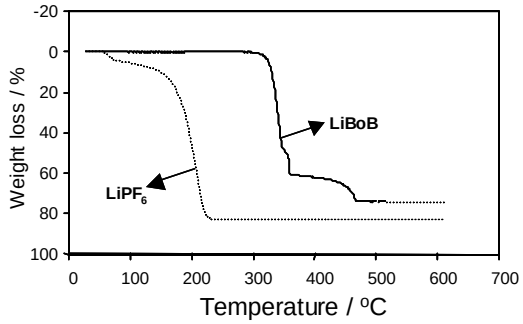

Fig. 4. Thermogravimetric analysis curves of LiBoB (solid line) and $LiPF_6$ (dotted line).

tant to develop an alternative electrolyte system that does not produce an acidic environment, so that the initial Mn dissolution (step I) does not occur.

Recently, lithium bisoxalatoborate (LiBoB, $LiB(C_2O_4)_2$) was synthesized and proposed as an alternative lithium salt for Li-ion cells [10,11]. Although the solubility and ambient-temperature ionic conductivity of LiBoB in relevant non-aqueous solvents are reported to be inferior to those of $LiPF_6$-based electrolyte systems [11], the absence of fluorine in the chemical structure of LiBoB has led us to consider it as an attractive Li salt for the LMOS/graphite Li-ion cells. Furthermore, our preliminary studies revealed that LiBoB possesses much better thermal stability than $LiPF_6$, as is shown in Fig. 4.

To investigate the possible use of the LiBoB-based electrolyte with the LMOS/graphite system, we first performed a Mn-dissolution experiment by mixing the spinel powder with the LiBoB-based electrolyte and aging the mixture at 55 °C for 4 weeks. Fig. 5 shows the concentration of Mn ions in the electrolyte after a 4-week storage of the SLMOS and stoichiometric $LiMn_2O_4$ powders in 1 M LiBoB/EC:DEC

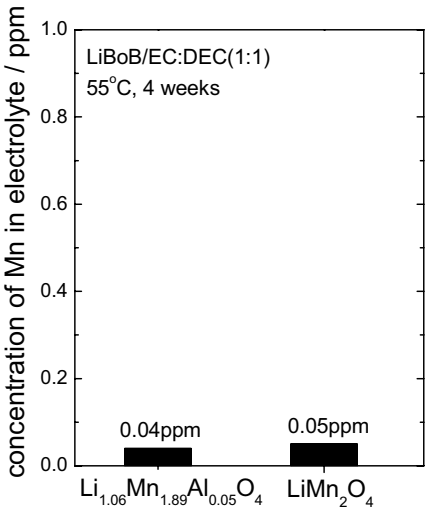

Fig. 5. Concentration of Mn dissolved from SLMOS and $LiMn_2O_4$ powders stored in 1 M LiBoB/EC:DEC (1:1) electrolyte at 55 °C after 4 weeks.

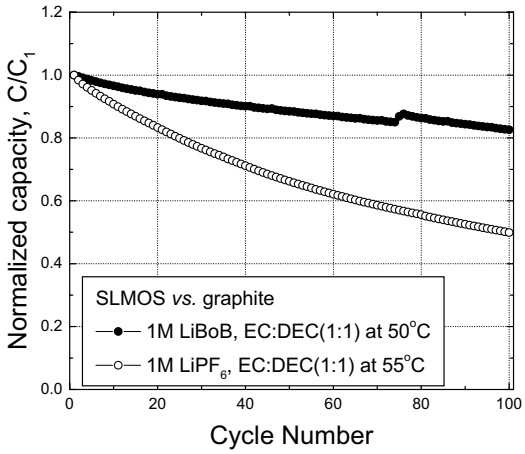

Fig. 6. Normalized discharge capacity against cycle number of SLMOS/graphite cells using 1 M LiBoB/EC:DEC (1:1) electrolyte (closed circles) and using 1 M $LiPF_6$/EC:DEC (1:1) electrolyte (open circles). C_1 denotes the first discharge capacity.

(1:1) at 55 °C. The Mn dissolution in the LiBoB-based electrolyte from both SLMOS and $LiMn_2O_4$ powders was very negligible (below the detection limit of ICP). Therefore, there is no need of stabilizing the spinel with LiBoB electrolyte, since no dissolution is taking place in both stabilized and stoichiometric spinels.

The cycling characteristics of cells using the LiBoB electrolyte system was then investigated. Fig. 6 shows the discharge capacity characteristics during the galvanostatic cycling of the SLMOS/graphite cell using 1 M LiBoB/EC:DEC (1:1) electrolyte and a similar cell using $LiPF_6$-based electrolyte at 50 °C. The results indicate that the Li-ion cell using the LiBoB-based electrolyte showed superior capacity retention (83% of the initial capacity after 100 cycles) compared with the one using the $LiPF_6$-based electrolyte. The improved cycling performance of the cell using the 1 M LiBoB/EC:DEC (1:1) electrolyte is attributed to the absence of fluorine in the chemical structure of LiBoB, so that no HF is produced and the Mn dissolution is suppressed, as was observed in Fig. 6.

Figs. 7 and 8 show the cell impedance and capacity characteristics during 55 °C aging and the DSC curve of fully charged SLMOS in the presence of a 1 M LiBoB/EC:DEC (1:1) electrolyte, respectively. No significant impedance rise and capacity fade with aging time were observed (Fig. 7). Also, a DSC curve of a fully charged spinel in the LiBoB-based electrolyte exhibited very limited thermal reactivity (Fig. 8), thus reflecting the superior thermal behavior of cells based on the spinel system.

Results presented in Figs. 6–8 indicate that the LiBoB-based electrolyte is quite promising for LMOS/graphite-based Li-ion batteries that can provide excellent calendar life and better abuse tolerance. However, for high-power applications, the impedance of the cell needs to be improved further to obtain better power capabilities when using the LiBoB-based electrolyte. One of the drawbacks of

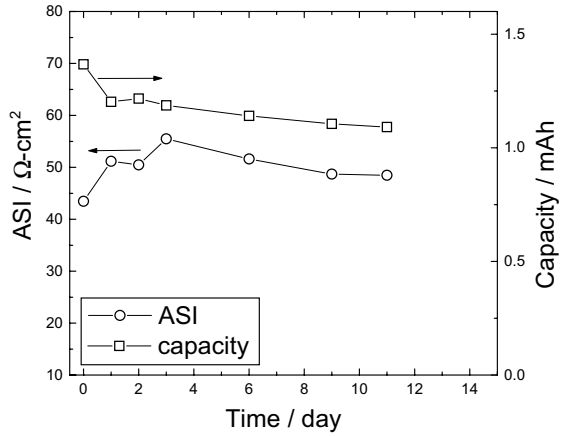

Fig. 7. Changes in ASI (open circles) and capacity (open squares) during 55 °C aging of SLMOS/graphite cell using 1 M LiBoB/EC:DEC (1:1) electrolyte.

the LiBoB-based electrolyte is its limited solubility in most linear carbonates, which usually provide low-viscosity electrolytes. Our first aim was to investigate the ASI of spinel cells having an EC- and DEC-based LiBoB electrolyte. The initial ASI of the cell using 1 M LiBoB/EC:DEC (1:1) electrolyte was higher than 40 Ω cm^2 (Fig. 7), whereas that of similar cells using 1 M $LiPF_6$/EC:DEC (1:1) was ∼28 Ω cm^2 [12,13]. For the Li-ion cells to power HEVs, the ASI should be below 35 Ω cm^2 at room temperature. Therefore, there is a need for developing an optimum electrolyte configuration based on LiBoB salt to get sufficient power capability for application in HEVs. To increase the lithium-ion conductivity of the LiBoB-based electrolyte system, we tested various organic solvents and solvent combinations. Among the organic solvents that show the best result was the 1:1:3 mixture of EC:PC:DMC. Fig. 9 shows the lithium-ion conductivity of EC:PC:DMC (1:1:3) with various concentrations of LiBoB salt. The composition that exhibits the highest lithium-ion conductivity as well as suitable viscosity was 0.7 M LiBoB/EC:PC:DMC (1:1:3). Based on the conductivity data shown in Fig. 9, we constructed a fixture cell with SLMOS, graphite, and 0.7 M LiBoB/EC:PC:DMC (1:1:3) as the cathode, anode, and electrolyte, respectively. We then

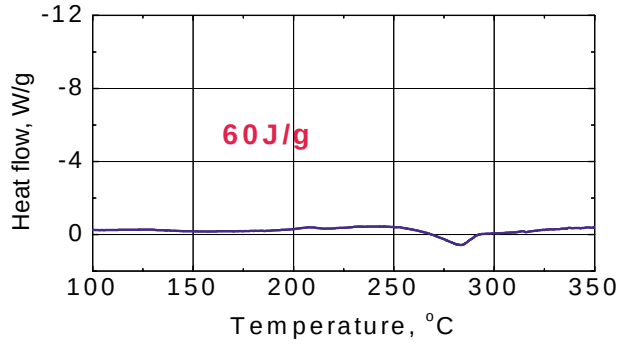

Fig. 8. DSC curve of fully charged SLMOS with 1 M LiBoB/EC:DEC (1:1) electrolyte. Heating rate was 10 °C/min.

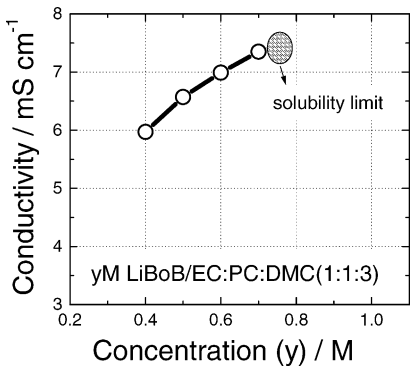

Fig. 9. The room-temperature lithium-ion conductivity of the 1:1:3 mixture of EC:PC:DMC with various concentrations of LiBoB salt.

performed the HPPC test at a 30 C pulse current rate. Fig. 10 shows that the cell ASI is about 25 and 18 Ω cm^2 for the 18 s pulse discharge and the 2 s regenerative pulse charge, respectively. These results exceed by far the power requirements set by the FreedomCAR for HEV applications (35 and 25 Ω cm^2, respectively). This result indicates that the lithium manganese oxide spinel, combined with LiBoB-based electrolyte, could provide high-power Li-ion batteries with low cost, good calendar life, and excellent thermal safety for HEV applications. More extensive work is under way to establish the long-term calendar life, safety, and power capabilities of the lithium manganese oxide spinel/LiBoB-based electrolyte/graphite Li-ion system. For the low temperature performance, the FreedomCAR has set a power requirement for cold cranking (−30 °C) at 7 kW. This requirement is very challenging even for $LiPF_6$-based electrolyte when using the nickel cobalt oxide system. We expect that LiBoB-based electrolyte may have the same problem. Further study is needed to carry out a phase diagram of LiBoB salt with different solvent configurations to determine the low temperature performance of LiBoB-based electrolytes and the solubility limit of this salt in the electrolytes at low temperature.

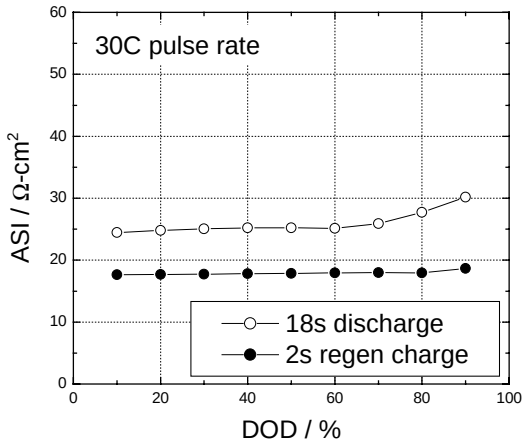

Fig. 10. The area-specific impedance (ASI) of SLMOS/graphite with 0.7 M LiBoB/EC:PC:DMC (1:1:3) as a function of depth of discharge (DOD). The pulse current rate was 30 °C.

4. Summary and conclusions

In spite of the very limited Mn dissolution of stabilized lithium manganese oxide spinel (SLMOS) in the $LiPF_6$-based electrolyte and good cycling performance versus the Li-metal anode, the SLMOS was found to still suffer from severe capacity fading when cycled in full Li-ion cells (versus graphite). The ac impedance data measured with the reference electrode cell revealed that the impedance of the graphite anode, which was much lower initially than that of the spinel cathode, significantly increased to overwhelm the latter after 55 °C cycling. The impedance data from the RE cell indicated that the increase in the interfacial resistance of the graphite anode is the main source of the cell degradation. We suggest the following successive processes as the possible degradation mechanism: (1) disproportionation and dissolution of Mn ions from the spinel powder into the electrolyte due to HF attack generated by fluorine from PF_6^- and protons from water impurities, (2) migration of the dissolved Mn ions to the graphite anode, (3) reduction of the Mn ions on the anode surface due to the chemical activity of the graphite, and (4) increase of charge-transfer impedance at the graphite/electrolyte interface.

Lithium bisoxalatoborate (LiBoB, $LiB(C_2O_4)_2$) was investigated as an alternative Li salt to $LiPF_6$ for a non-aqueous electrolyte for use with the lithium manganese oxide spinel/graphite Li-ion cells. The Li-ion cells employing the LiBoB-based electrolyte exhibited superior performance relative to the cells with $LiPF_6$-based electrolyte. This included (a) good high-temperature cycling performance, (b) lower thermal reactivity of the charged cathode with electrolyte, and (c) better accelerated aging characteristics. The improved performance of the cells with LiBoB-based electrolyte was attributed to the chemical structure of the LiBoB salt that does not contain any fluorine, so that no HF is produced by salt decomposition. As a result, almost no Mn dissolution, from spinel powder when exposed to LiBoB-based electrolyte, was detected after high-temperature storage. Through optimization of organic solvents to increase the lithium-ion conductivity of the electrolyte system, we developed lithium manganese oxide spinel/graphite with a 0.7 M LiBoB in EC:PC:DMC (1:1:3) system that shows far better power performance than that required by FreedomCAR. In conclusion, lithium manganese oxide spinel/LiBoB-based electrolyte/graphite high-power Li-ion cells are very promising energy storage systems for HEV applications with longer calendar life, better safety, and lower cost.

Acknowledgements

The authors acknowledge the financial support of the US Department of Energy, FreedomCAR & Vehicle Technologies Program, under Contract no. W-31-109-Eng-38. Also, the authors are very grateful for the continued support of their DOE sponsor, Mr. Tien Duong. Also, the authors wish to thank Dr. Richard Jow for valuable discussions.

References

[1] C.H. Chen, J. Liu, M.E. Stoll, G. Henriksen, D.R. Vissers, K. Amine, J. Electrochem. Soc., in press.
[2] D.H. Jang, Y.J. Shin, S.M. Oh, J. Electrochem. Soc. 143 (1996) 2204.
[3] D.H. Jang, S.M. Oh, J. Electrochem. Soc. 144 (1997) 3342.
[4] A. Du Pasquier, A. Blyr, P. Courjal, D. Larcher, G. Amatucci, B. Gerand, J.-M. Tarascon, J. Electrochem. Soc. 146 (1999) 428.
[5] D.P. Abraham, J. Liu, C.H. Chen, Y.E. Hyung, M. Stoll, N. Elsen, S. MacLaren, R. Twesten, R. Haasch, E. Sammann, I. Petrov, K. Amine, G. Henriksen, J. Power Sources 119 (2003) 511.
[6] S.-H. Kang, J. Kim, M.E. Stoll, D. Abraham, Y.K. Sun, K. Amine, J. Power Sources 112 (2002) 41.
[7] G. Pistoia, A. Antonini, R. Rosati, C. Bellitto, G.M. Ingo, Chem. Mater. 9 (1997) 1443.
[8] A. Blyr, C. Sigala, G.G. Amatucci, D. Guyomard, Y. Chabres, J.M. Tarascon, J. Electrochem. Soc. 145 (1998) 194.
[9] U. Lishka, U. Wietelmann, M. Wegner, German Patent DE19829030 C1 (1999).
[10] W. Xu, C.A. Angell, Electrochem. Solid-State Lett. 4 (2001) E1.
[11] K. Xu, S. Zhang, T.R. Jow, W. Xu, C.A. Angell, Electrochem. Solid-State Lett. 5 (2002) A26.
[12] K. Amine, J. Liu, in: Proceedings of the First International Conference on Polymer Batteries and Fuel Cells, Jeju, Korea, 1–6 June, 2003, p. INV 14 (extended abstract).
[13] K. Amine, J. Liu, Y. Hyung, I. Belharouak, G. Henriksen, in: Proceedings of the 43rd Battery Symposium in Japan, Fukuoka, Japan, 12–14 October, 2003, p. 2 (extended abstract).